Extraction of axial form factors from $\bar{B}^0 \to D^+ K^- K^{*0}$ decay

Chun-Khiang Chua
Institute of Physics, Academia Sinica, Taipei, Taiwan 115, Republic of China

Wei-Shu Hou and Shang-Yuu Tsai
Department of Physics, National Taiwan University, Taipei, Taiwan 106, Republic of China

(Received 4 May 2004; published 31 August 2004)

Based on $\bar{B} \to D^{(*)} K^- K^{*0}$ decay data, which supports factorization, we propose to extract the kaon axial form factor in the factorization framework. Experiment indicates that the $K^- K^{*0}$ pair is produced by an axial current where only one out of three axial form factors is dominant. The axial form factor can be extracted by fitting the $K^- K^{*0}$ mass spectrum with an $a_1(1260)$-resonance plus QCD-motivated nonresonant contributions, which can be improved as data improves.

DOI: 10.1103/PhysRevD.70.034032 PACS number(s): 13.25.Hw, 14.40.Nd

I. INTRODUCTION

The three-body $\bar{B} \to D K^- K^{*0}$, $D^* K^- K^{*0}$ and $\bar{B} \to D K^- K^0$, $D^* K^- K^0$ decays were observed for the first time by the Belle Collaboration based on 29.4 fb^{-1} of data [1]. For the $\bar{B} \to D^{(*)} K^- K^{*0}$ channels, one has a peak near threshold in the $K^- K^{*0}$ mass spectrum, which can be described by a dominant $a_1(1260)$ resonance contribution; although there is a possible peak at ~ 2 GeV. In addition, angular analysis finds $K^- K^{*0}$ to be in the $J^P = 1^+$ configuration, supporting the $a_1(1260)$ pole dominance picture. The fitted parameters, however, give larger $a_1^-(1260) \to K^- K^{*0}$ branching fraction [1], by a factor of 2 or more, than what is obtained from the three pion mass spectrum in τ decays [2].

The peaking near threshold of the $K^- K^{*0}$ mass spectrum suggests a *quasi-two-body* process where the collinear $K^- K^{*0}$ pair recoils against the $D^{(*)}$ meson. This suggests that factorization could be at work for such three-body decays. In our previous work on $\bar{B}^0 \to D^{(*)+} K^- K^{(*)0}$ and $B^- \to D^{(*)0} K^- K^{(*)0}$ decays, two kinds of decay amplitudes arose due to different flavor structures that give rise to the $D^{(*)}$ meson [3]. The $\bar{B}^0 \to D^{(*)+} K^- K^{(*)0}$ process involves only the matrix element $\langle K^- K^{(*)0} | V-A | 0 \rangle$, where the $K^- K^{(*)0}$ is produced by a weak $V-A$ current. For $B^- \to D^{(*)0} K^- K^{(*)0}$, one has in addition a $\langle K^- K^{(*)0} | V-A | B^- \rangle$ contribution, where B^- goes into $K^- K^{(*)0}$ via a weak current.

Under factorization, the $\bar{B}^0 \to D^{(*)+} K^- K^0$ decay amplitude is a product [Fig. 1(a)] of the matrix elements $\langle K^- K^0 | V-A | 0 \rangle$ and $\langle D^{(*)+} | V-A | \bar{B}^0 \rangle$. From parity, $K^- K^0$ can only be produced by the vector current in $\langle K^- K^0 | V-A | 0 \rangle$, which carries both $J^P = 0^+$ and 1^- components. The $K^- K^0$ pair, however, should dominantly be in the 1^- state by isospin symmetry. This is consistent with experiment, which finds $K^- K^0$ dominantly in 1^- [1,4]. By using isospin rotation, the kaon weak form factor $\langle K^- K^0 | V | 0 \rangle$ can be further related to the kaon electromagnetic (EM) form factors in $e^+ e^-$ annihilation, where much data exist. Without tuning parameters, we obtained the value for $\mathcal{B}(\bar{B}^0 \to D^{(*)+} K^- K^0)$, which is in good agreement with experiment [3]. The predicted $K^- K^0$ mass spectrum has a peak near threshold as a consequence of the kaon form factor, which can be checked by experiment. The prediction of $K^- K^0$ to be in the 1^- state and good agreement with the observed branching fraction gives strong support for factorization in $\bar{B}^0 \to D^{(*)+} K^- K^0$ decay.

As illustrated in Fig. 1, $\bar{B}^0 \to D^{(*)+} K^- K^0$ decay bears some similarity with the baryonic $B^0 \to D^{*-} p \bar{n}$ decay, which was first measured by the CLEO Collaboration [5]. Under factorization, the $B^0 \to D^{*-} p \bar{n}$ decay amplitude contains [6] the matrix element $\langle p \bar{n} | V-A | 0 \rangle$, which involves both vector and axial current form factors. We had also used isospin to relate the vector current form factor to the EM data. It was found that the vector current contribution could account for $\sim 60\,\%$ of the observed rate [6]. The predicted $p \bar{n}$ mass spectrum also exhibits near threshold enhancement. Unfortunately, this mass spectrum cannot be checked immediately. Furthermore, there is no data on axial current baryon form

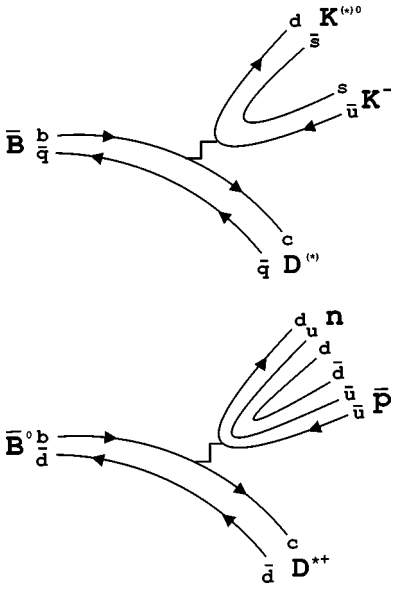

FIG. 1. (a) The $K^- K^{(*)0}$ and (b) $\overline{p n}$ pairs produced by a current. The wavy line is the W boson.

factors. We suggested instead that one could perform an inverse transform to obtain nucleon axial form factors once the B decay data becomes available. It would be interesting if fundamental quantities, such as nucleon axial form factors, can be extracted directly from B physics data. It should be noted that $\bar{B}^0 \to D^{(*)0} p\bar{p}$ spectra have been measured [7] and the a_1-pole contribution could be important [8]. However, we cannot use them to obtain nucleon axial form factors, since these modes are dominated by transition contributions, i.e., $\mathcal{A} \propto \langle p\bar{p}|j|\bar{B}^0\rangle \langle D^{(*)0}|j|0\rangle$, in the factorization approach.

Unlike the $B^0 \to D^{*-} p\bar{n}$ case, we already have some data of the $K^- K^{*0}$ mass spectrum for the $\bar{B} \to D^{(*)} K^- K^{*0}$ decay. In the factorization framework, the $K^- K^{*0}$ pair in $\bar{B}^0 \to D^{(*)+} K^- K^{*0}$ can be produced by both vector and axial currents. However, experiment found that $K^- K^{*0}$ is dominantly in $J^P = 1^+$ configuration, implying a dominant axial current contribution. By neglecting contributions from the vector and the timelike component of the axial current (which would give 0^-), it is possible to obtain the timelike K^--K^{*0} axial form factors from $\bar{B}^0 \to D^{(*)+} K^- K^{*0}$ decay data.

In this paper, our purpose is to demonstrate the extraction of the axial form factor from data. Unfortunately, although more data is already available, at present the $K^- K^{*0}$ mass spectrum is given only by combining $D^+ K^- K^{*0}$, $D^{*+} K^- K^{*0}$, $D^0 K^- K^{*0}$, and $D^{*0} K^- K^{*0}$ modes. To stimulate further experimental studies, we generate mock data based on the existing one, from which an inverse transform is done to obtain the axial form factor. In Sec. II we formulate the factorization approach and define the K^--K^{*0} axial form factors. The implications of angular analysis on the form factors will be examined, and the form factor is then parametrized for subsequent use. The fit results to mock data are obtained in Sec. III, which is followed by discussion and conclusion in Sec. IV.

II. FORMULATION

The relevant effective Hamiltonian is

$$\mathcal{H}_{\rm eff} = \frac{G_F}{\sqrt{2}} V_{cb} V_{ud}^* [c_1(\mu) \mathcal{O}_1^c(\mu) + c_2(\mu) \mathcal{O}_2^c(\mu)], \quad (1)$$

where $c_i(\mu)$ are the Wilson coefficients and V_{cb} and V_{ud} are the Cabibbo-Kobayashi-Maskawa (CKM) matrix elements. The operators $\mathcal{O}_i$ are products of $V-A$ currents, i.e., $\mathcal{O}_1^c = (\bar{c}b)_{V-A} (\bar{d}u)_{V-A}$ and $\mathcal{O}_2^c = (\bar{d}b)_{V-A} (\bar{c}u)_{V-A}$, where $(\bar{q}q')_{V-A} \equiv \bar{q}\gamma^\mu (1-\gamma^5) q'$.

We concentrate on the $\bar{B}^0 \to D^+ K^- K^{*0}$ decay mode, since under factorization it involves only a simple $\bar{B}^0 \to D^+$ transition and $\langle K^- K^{*0}|V-A|0\rangle$, giving the decay amplitude

$$\mathcal{A}(D^+ K^- K^{*0}) = \frac{G_F}{\sqrt{2}} V_{cb} V_{ud}^* a_1 \langle D^+|(\bar{c}b)_{V-A}|\bar{B}^0\rangle \times \langle K^- K^{*0}|(\bar{d}u)_{V-A}|0\rangle, \quad (2)$$

where $a_1 \equiv c_1 + c_2/N_c$ with N_c the effective number of colors if naïve factorization is used. In practice, we may need to use the a_1 coefficient fitted from $\bar{B} \to D a_1$ decays. The matrix element $\langle D^+|(\bar{c}b)_{V-A}|\bar{B}^0\rangle$ is the same as in two-body decay, and is parametrized by

$$\langle D^+(p_D)|V^\mu|\bar{B}^0(p_B)\rangle = \left(g^{\mu\nu} - \frac{q^\mu q^\nu}{q^2}\right)(p_B + p_D)_\nu F_1^{BD}(q^2) + \frac{m_B^2 - m_D^2}{q^2} q^\mu F_0^{BD}(q^2), \quad (3)$$

where $q \equiv p_B - p_D = p_K + p_{K^*}$. We employ the Melikhov-Stech (MS) model [9] for the form factors F_0^{BD} and F_1^{BD}. For $\langle K^- K^{*0}|(\bar{d}u)_{V-A}|0\rangle$, since $K^- K^{*0}$ is produced by the V and A currents, in the $K^- K^{*0}$ rest frame, the allowed angular momentum and parity configurations for $K^- K^{*0}$ are $J^P = 0^-$, 1^+ and 1^-, which transform in the same way as the axial vector current A^μ $(0^-, 1^+)$ and the spatial part of the vector current V^i (1^-), respectively. A convenient parametrization that manifests the possible J^P configurations is then given by

$$\begin{aligned} i\langle K^-(p_K) K^{*0}(p_{K^*}, \varepsilon_{K^*})|(V-A)_\mu|0\rangle &= i\epsilon_{\mu\nu\alpha\beta} \varepsilon_{K^*}^{*\nu} p_K^\alpha p_{K^*}^\beta \frac{2V(q^2)}{m_K + m_{K^*}} + \left(g_{\mu\nu} - \frac{q_\mu q_\nu}{q^2}\right) \varepsilon_{K^*}^{*\nu} \\ &\times (m_K + m_{K^*}) A_1(q^2) - \left(g_{\mu\nu} - \frac{q_\mu q_\nu}{q^2}\right) \\ &\times (p_K - p_{K^*})^\nu (\varepsilon_{K^*}^* \cdot q) \frac{A_2(q^2)}{m_K + m_{K^*}} \\ &+ \frac{2m_{K^*}}{q^2} q_\mu (\varepsilon_{K^*}^* \cdot q) A_0(q^2), \end{aligned} \quad (4)$$

where the form factors V, A_0 and A_1, A_2 are induced, in the $K^- K^{*0}$ rest frame, by the vector V^i (1^-), the timelike component of the axial vector $A^{\mu=0}$ (0^-) and the spacelike component of the axial vector currents A^i (1^+), respectively. It should be noted that once factorized, the angular-momentum quantum number of the $K^- K^{*0}$, hence the allowed resonances, can only be $J = 0, 1$ to match the current. Any $K^- K^{*0}$ or intermediate resonance component with $J > 1$ cannot be accommodated [4] within factorization approach.

Upon squaring the amplitude of Eq. (2), the decay rate would involve interference between the four form factors of $\langle K^- K^{*0}|V-A|0\rangle$. Simply knowing the $K^- K^{*0}$ mass spectrum is far from being sufficient to constrain all the parameters. One thus needs further experimental input. Since we have parametrized $\langle K^- K^{*0}|V-A|0\rangle$ in accordance with the angular-momentum configuration of the $K^- K^{*0}$, it is straightforward to see what information can be gained by studying the angular distributions.

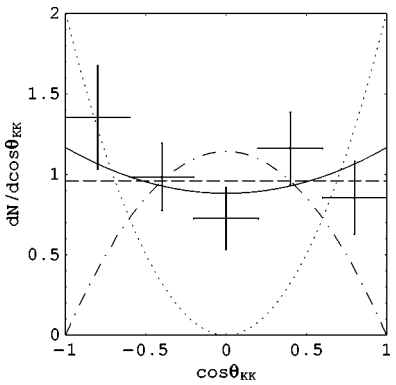

FIG. 2. Fit to angular distribution by $a(1+b\cos^2\theta_{KK})$ (solid), a constant c (dash), $\xi\sin^2\theta_{KK}$ (dash-dot), and $\zeta\cos^2\theta_{KK}$ (dot), with $(a,b,\chi^2/N_{\rm DF})=(0.88,0.32,3.5/3)$, $(c,\chi^2/N_{\rm DF})=(0.99,4.0/4)$, $(\xi,\chi^2/N_{\rm DF})=(1.14,18.2/4)$, and $(\zeta,\chi^2/N_{\rm DF})=(2.0,39.3/4)$, respectively (where N_{DF} stands for Number of degrees of freedom). The $\cos^2\theta_{KK}$ and $\sin^2\theta_{KK}$ distributions are clearly disfavored by data.

Denoting $\mathbf{p}_h^*$ the three-momentum of meson h in the K^-K^{*0} rest frame, and $\mathbf{p}_h$ in the $\bar{B}^0$ rest frame, the helicity angle θ_{KK} is defined as the angle between $\mathbf{p}_{K*}^*$ and $-\mathbf{p}_D$ [1]. The angular distributions coming from V^i (1^-) and $A^{\mu=0}$ (0^-) are

$$\frac{d\Gamma_V}{d\cos\theta_{KK}}\propto\sin^2\theta_{KK}, \tag{5}$$

$$\frac{d\Gamma_{A_0}}{d\cos\theta_{KK}}\propto\text{constant}, \tag{6}$$

respectively, where we have used V and A_0 to denote the corresponding contributions. Likewise, for A^i (1^+), we have

$$\frac{d\Gamma_{A_1}}{d\cos\theta_{KK}}\propto 1+b\cos^2\theta_{KK}, \tag{7}$$

$$\frac{d\Gamma_{A_2}}{d\cos\theta_{KK}}\propto\cos^2\theta_{KK}, \tag{8}$$

$$\frac{d\Gamma_{A_1A_2^*}}{d\cos\theta_{KK}}\propto\cos^2\theta_{KK}, \tag{9}$$

from A_1, A_2 and their interference, respectively.

As shown in Fig. 2, the data points scatter around the horizontal line $dN/d\cos\theta_{KK}\sim 1$. One concludes that the V (1^-) and A_2 contributions are not favored by present data and can be safely dropped at this stage. On the other hand, angular analysis of subsequent $K^*\to K\pi$ decay suggests K^-K^{*0} is dominantly 1^+ [1], therefore, preferring A_1 over A_0.

It is interesting to understand how A_1, with $d\Gamma_{A_1}/d\cos\theta_{KK}\propto 1+b\cos^2\theta_{KK}$, can describe the data in Fig. 2, which seems quite consistent with a constant distribution. From

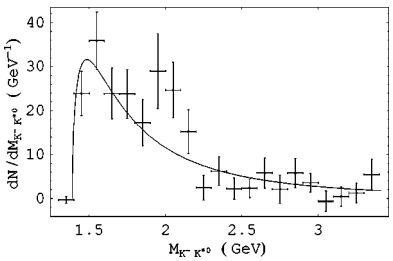

FIG. 3. The observed [1] K^-K^{*0} mass spectrum combining $D^+K^-K^{*0}$, $D^{*+}K^-K^{*0}$, $D^0K^-K^{*0}$, and $D^{*0}K^-K^{*0}$ modes. The experimental fit in Ref. [1] assumes only the $a_1(1260)$ resonance. The $\chi^2/N_{\rm DF}$ is $\sim$24/18 and the obtained nominal width of $a_1(1260)$ is 380 MeV.

$$\frac{d\Gamma_{\rm tot}}{d\cos\theta_{KK}}\approx\frac{d\Gamma_{A_1}}{d\cos\theta_{KK}}$$

$$\propto\int dM_{KK*}|\mathbf{p}_{K*}^*||\mathbf{p}_D|(F_1^{BD})^2|A_1|^2\mathbf{p}_D^{*2}$$

$$\times\left(1+\frac{\mathbf{p}_{K*}^{*2}}{m_{K*}^2}\cos^2\theta_{KK}\right) \tag{10}$$

$$\propto a(1+b\cos^2\theta_{KK}), \tag{11}$$

where $M_{KK*}^2\equiv q^2$. We find that b in Eq. (11) is *small* due to the factor $\mathbf{p}_{K*}^{*2}$ in Eq. (10) as a consequence of threshold peaking, resulting in a flattened parabola which mimics a constant. We reproduce the experimental data in Fig. 3, where one can see a clear threshold peak while large $t\equiv M_{KK*}^2$ is suppressed. The major part of the rate comes from the low M_{KK*} region, resulting in a suppressed $\mathbf{p}_{K*}^{*2}$ in KK^* frame. For higher M_{KK*} where $\mathbf{p}_{K*}^{*2}$ is large, the contribution to b is suppressed by the tail of the K^-K^{*0} mass spectrum.

It should be emphasized that, although the present data disfavor any significant contributions from V, A_2, and A_0, it is possible that these contributions, however small, may show up in the future when one has sufficient amount of data. It is clear, however, that one can always use angular analysis to project out each form factor. As this is not yet the case, for this work we concentrate only on the dominant $A_1(q^2)$ term and neglect terms involving other form factors. The $\bar{B}^0\to D^+K^-K^{*0}$ decay amplitude can now be simplified to

$$\mathcal{A}(D^+K^-K^{*0})=-i\frac{G_F}{\sqrt{2}}V_{cb}V_{ud}^*a_1F_1^{BD}(q^2)A_1(q^2)$$

$$\times(m_K+m_{K*})2p_D\left(\varepsilon_{K*}^*-\frac{\varepsilon_{K*}^*\cdot q}{q^2}q\right). \tag{12}$$

As shown in Fig. 3 the data generally follows the experimental fit that assumes only the $a_1(1260)$ resonance, which we

have now generalized into the $A_1(q^2)$ form factor. Note that the second peak at $M_{KK^*}\sim 2$ GeV in the data has large statistical error and is dubious for lack of known resonances. In any case, it would require more data to clarify.

K^-K^{*0} can be produced via both resonant and nonresonant contributions. We parametrize the A_1 form factor by including a single $a_1(1260)$ resonance to account for the resonant contribution. For nonresonant contributions, we take cue from perturbative QCD (PQCD) [10], which states that at least one *hard* gluon is needed to redistribute the large momentum transfer t in K^-K^{*0}. We then follow [6] and expand in $1/t^n$ for the nonresonant part, with n starting at 1 to reflect this hard gluon exchange. For simplicity, and since data is still scarce at present, we take just two terms ($n=1,\ 2$). We further impose a 180° difference between the phases of the complex expansion coefficients. This is to compensate for the (possibly) artificial rise at low t from the leading $1/t$ term. Such alternative signs are seen in the fits of nucleon EM form factors [6]. The nonresonant phases are taken as constant. The A_1 form factor is then parametrized as

$$A_1(t)=\frac{g_s m_{a_1} f_{a_1}}{t-m_{a_1}^2+i m_{a_1}\Gamma(t)} + e^{i\phi}\left(\frac{x_1}{t}-\frac{x_2}{t^2}\right)\left[\ln\left(\frac{t}{0.3^2}\right)\right]^{-1}, \tag{13}$$

where m_{a_1}, f_{a_1} are, respectively, the mass and decay constant of $a_1(1260)$, g_s the $a_1(1260)\to KK^*$ coupling constant, and $x_{1,2}$ and ϕ are the strengths and phase of the nonresonant terms.

The $a_1(1260)$ is broad and the width is not yet well known and could range anywhere between 250 to 600 MeV [11]. It is not appropriate to treat the total width as constant, which is only valid in narrow-width approximation. We use [1],

$$\Gamma(t)=\Gamma_{a_1}\frac{\rho_{\rho\pi}(t)}{\rho_{\rho\pi}(m_{a_1}^2)}, \tag{14}$$

where the constant Γ_{a_1} is the nominal width of $a_1(1260)$, and

$$\rho_{\rho\pi}\equiv\left(1+\frac{\mathbf{p}_{\boldsymbol{\rho}}^{*2}}{3m_\rho^2}\right)|\mathbf{p}_{\boldsymbol{\rho}}^*|, \tag{15}$$

where, in addition to the phase space factor $|\mathbf{p}_{\boldsymbol{\rho}}^*|$ similar to what is used in [1], we also take into account the amplitude squared of $a_1(1260)\to(\rho\pi)_{s-\text{wave}}$. The total width of $a_1(1260)$ is approximated by the $a_1(1260)\to(\rho\pi)_{s-\text{wave}}$ partial width.

The branching fraction of $a_1^-(1260)\to K^-K^{*0}$ can be extracted by taking the ratio of the areas under the spectral functions of $a_1^-(1260)\to$ all [approximated by $a_1\to(\rho\pi)_{s-\text{wave}}$] and $a_1^-(1260)\to K^-K^{*0}$, respectively

$$\Pi_{\rho\pi}\equiv\frac{m_{a_1}\Gamma_{a_1}}{\pi}\frac{\Gamma(t)}{(t-m_{a_1}^2)^2+m_{a_1}^2\Gamma(t)^2}, \tag{16}$$

$$\Pi_{KK^*}\equiv\frac{m_{a_1}\Gamma_{a_1}}{\pi}\frac{\Gamma_{KK^*}(t)}{(t-m_{a_1}^2)^2+m_{a_1}^2\Gamma(t)^2}, \tag{17}$$

where the partial width of $a_1(1260)\to K^-K^{*0}$ is given by

$$\Gamma_{KK^*}(t)\equiv\left[\frac{g_s^2(m_K+m_{K^*})^2}{8\pi}\frac{\rho_{\rho\pi}(m_{a_1}^2)}{m_{a_1}^2}\right]\frac{\rho_{KK^*}(t)}{\rho_{\rho\pi}(m_{a_1}^2)}, \tag{18}$$

and

$$\rho_{KK^*}\equiv\left(1+\frac{\mathbf{p}_{\mathbf{K^*}}^{*2}}{3m_{K^*}^2}\right)|\mathbf{p}_{\mathbf{K^*}}^*|.$$

Comparing to the definition of $\Gamma(t)$, the constant inside the brackets of Eq. (18) plays the same role as that of Γ_{a_1} in Eq. (14), i.e., the nominal value of the partial width of $a_1^-(1260)\to K^-K^{*0}$. In the narrow width limit, $\Gamma_{a_1}\to 0$, we recover

$$\frac{1}{(t-m_{a_1}^2)^2+m_{a_1}^2\Gamma(t)^2}\approx\frac{\pi}{m_{a_1}\Gamma_{a_1}}\delta(t-m_{a_1}^2),$$

such that

$$\Pi_{\rho\pi}\approx\Gamma(m_{a_1}^2)\,\delta(t-m_{a_1}^2)=\Gamma_{a_1}\delta(t-m_{a_1}^2), \tag{19}$$

$$\Pi_{KK^*}\approx\Gamma_{KK^*}(m_{a_1}^2)\,\delta(t-m_{a_1}^2), \tag{20}$$

for $\Gamma_{a_1}\to 0$. Since in reality $m_{KK^*}>m_{a_1}$ the "branching fraction" R of $a_1^-(1260)\to K^-K^{*0}$ is then defined by

$$R\equiv\frac{\int_{(m_K+m_{K^*})^2}^{\infty}\Pi_{KK^*}(t)dt}{\int_{(m_K+m_{K^*})^2}^{\infty}\Pi_{KK^*}(t)dt+\int_{(m_\rho+m_\pi)^2}^{\infty}\Pi_{\rho\pi}(t)dt}. \tag{21}$$

Our method for extracting the $a_1^-(1260)\to K^-K^{*0}$ rate is similar to the one used by the CLEO Collaboration in Ref. [2]. In the fit to $\tau^-\to\nu_\tau\pi^-\pi^0\pi^0$, which is dominated by $\tau^-\to\nu_\tau a_1^-(1260)$, the $a_1^-(1260)\to K^-K^{*0}$ "rate" ($R_{\text{CLEO}}\sim 3\,\%$) was extracted by taking into account $a_1^-(1260)\to K^-K^{*0}$ and other processes that may contribute to the $a_1(1260)$ Breit-Wigner width. This is in contrast with the way the result was obtained in Ref. [1], where the $a_1(1260)$ was thought to account for the whole spectrum, and the corresponding factor R_{Belle} is obtained by using $R_{\text{Belle}}\equiv\mathcal{B}(\bar{B}^0\to D^+K^-K^{*0})/\mathcal{B}(\bar{B}^0\to D^+a_1^-(1260))\sim 15\,\%$. Only in the narrow width and $m_{a_1}>m_{KK^*}$ limit that R_{Belle} reduces to R defined in Eq. (21).

III. RESULTS

Throughout this paper, we use $a_1=0.935$, $m_{a_1}=1230$ MeV, $f_{a_1}=229$ MeV, and the CKM matrix elements $V_{ud}=0.975$, $V_{cb}=0.039$ as in Ref. [3].

The mass spectra plotted in Fig. 3 is taken from Ref. [1], which combines $D^+K^-K^{*0}$, $D^{*+}K^-K^{*0}$, $D^0K^-K^{*0}$, and $D^{*0}K^-K^{*0}$ modes. Our model parametrization in Sec. II, however, is constructed only for $D^+K^-K^{*0}$. Since our present purpose is only to demonstrate the feasibility of extracting the A_1 form factor from B decay data, we shall make our own *mock data* on which to practice the extraction.

Starting with Fig. 3, which is based on 29.4 fb^{-1} of data, we first transform from dN/dM_{KK^*} into $d\mathcal{B}/dM_{KK^*}$, normalized by the measured $\mathcal{B}(D^+K^-K^{*0})=[8.8\pm1.1(\text{stat})\pm1.5(\text{syst})]\times10^{-4}$ [1]. Since the KEKB accelerator has already accumulated over 150 million $B\overline{B}$ pairs ($\sim$140 fb^{-1}) by summer 2003, we take our mock data to be five times the original one ($\sim$29.4 fb^{-1}), i.e., $\sim$150 fb^{-1}, but keeping the central value for $\mathcal{B}(D^+K^-K^{*0})$ unchanged. Next, we refine the resolution in M_{KK^*} by rebinning two bins into three, again keeping the same central value and maintaining consistent statistical error.

The second peak at $M_{KK^*}\sim2$ GeV remains after rebinning, but no known resonances can account for it. We, therefore, *remove it by hand*. In order to do so, we first assume the data has a shape that roughly follows the curve given by some chosen set of parameters: $g_s=1.4$, $\Gamma_{a_1}=430$ MeV, $x_1=8$ GeV^2, $x_2=1$ GeV^4, and $\phi=-40°$, which give $\mathcal{B}(D^+K^-K^{*0})=8.4\times10^{-4}$ and $\chi^2/N_{\rm DF}=22.6/26$. The branching fraction R of $a_1^-(1260)\to K^-K^{*0}$ given by Eq. (21) is 4.3 %, which is small compared to the value (8–15 %) of Ref. [1]. With this curve as a guide, we remove the second peak, but respect the statistical error in the corresponding M_{KK^*} range.

Having generated the mock data, we then redo the fitting. The best fit with $\chi^2/N_{\rm DF}=19.2/26$ is obtained with the following:

$$g_s=2.41,\quad \Gamma_{a_1}=678\quad \text{MeV},\quad x_1=8.32\quad \text{GeV}^2,$$
$$x_2=3.07\ \text{GeV}^4,\quad \phi=-18.7°, \tag{22}$$

which give $\mathcal{B}(D^+K^-K^{*0})=8.33\times10^{-4}$, and a larger branching fraction $R=8.18$ % due to a larger strong coupling g_s. The fit result is shown in Fig. 4. The dominant contribution is from the nonresonant term, which gives $\sim$54 % of the rate. The $a_1(1260)$ resonance contributes only $\sim$9 % of the rate by itself, with the remaining $\sim$36 % arising from interference with the nonresonant term. The interference is constructive because the nonresonant phase $\phi=-18.7°$ lies in the same quadrant as the resonance phase $\tan^{-1}[-m_{a_1}\Gamma(t)/(t-m_{a_1}^2)]$, which varies between $-90°$ to $0°$ for $t\gtrsim m_{a_1}^2$.

In Fig. 5 we show the A_1 form factor with the parameters of Eq. (22). The relative sign between the real and imaginary parts of the form factor is mainly due to the phase $\phi=-18.7°$, which is coherent with the $a_1(1260)$ resonance

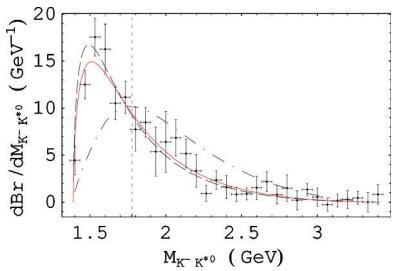

FIG. 4. $d\mathcal{B}/dM_{KK^*}$ (in units of 10^{-4}) mock data for $\overline{B}^0\to D^+K^-K^{*0}$ assuming five times ($\sim$150 fb^{-1}) the original data [1] of 29.4 fb^{-1}. The solid curve corresponds to Eq. (22). The dash curve is given by $g_s=1.4$, $\Gamma_{a_1}=430$ MeV, $x_{1(2)}=8(1)$ GeV$^{2(4)}$, and $\phi=-40°$. The dot-dash curve is given by $g_s=0.89$, $\Gamma_{a_1}=350$ MeV, $x_{1(2)}=23.2(38.2)$ GeV$^{2(4)}$, and $\phi=201°$. The vertical dot line indicates the τ mass.

phase, and gives a negative imaginary part. The x_1 term contributes $\sim$131 % to the nonresonant contribution and dominates A_1, compared to only $\sim$2 % from x_2, where we have built in destructive interference between x_1 and x_2 parts.

It is useful to investigate the χ^2 behavior in the vicinity of the best fit values of Eq. (22). We find that, within $\Delta\chi^2=1$, the χ^2 depends on g_s and Γ_{a_1} roughly via the ratio g_s/Γ_{a_1}, hence many "solutions" exist with differing a_1 width. This is because the rate is dominated by the near-threshold contribution where the $t-m_{a_1}^2$ factor in Eq. (13) is small compared to $m_{a_1}\Gamma(t)$, hence resulting in a resonance term that is roughly characterized by g_s/Γ_{a_1}. Since this is inherent in our form factor model, one cannot determine g_s and Γ_{a_1} separately even when the independent $\overline{B}^0\to D^+K^-K^{*0}$ spectrum has become available. One, therefore, needs independent input on $a_1(1260)$ resonance, which we discuss in Sec. IV.

IV. DISCUSSION AND CONCLUSION

We see that independent input on $a_1(1260)$ width is needed to extract the K-K^* axial A_1 form factor. To clarify this point further, we note that the $\tau\to\nu_\tau K^-K^{*0}$ process is very similar to $\overline{B}^0\to D^+K^-K^{*0}$, with $a_1V_{cb}\langle D^+|(V-A)^\mu|\overline{B}^0\rangle$ in Eq. (2) replaced by $\overline{u_{\nu_\tau}}\gamma^\mu(1-\gamma_5)u_\tau$. Factorization in this case is basically exact, and K^-K^{*0} production comes only from the axial current. By using the best fit val-

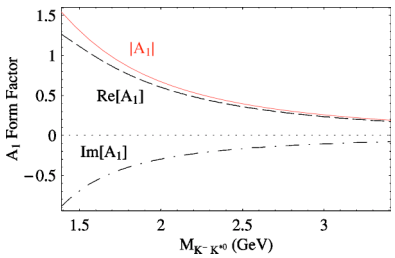

FIG. 5. Plot of $|A_1|$ (solid), Re$[A_1]$ (dash), and Im$[A_1]$ (dot-dash) from Eq. (22).

ues of Eq. (22), we obtain $\mathcal{B}(\tau\to\nu_\tau K^- K^{*0})=5.3\times 0^{-3}$ $\sim 0.5\,\%$, similar to Ref. [1], and is more than twice the measured rate of $(2.1\pm 0.4)\times 10^{-3}$ [11].

Our larger predicted $\tau\to\nu_\tau K^- K^{*0}$ rate can be understood as follows. Although both $\mathcal{B}(\bar{B}^0\to D^+ K^- K^{*0})$ and $\mathcal{B}(\tau\to\nu_\tau K^- K^{*0})$ are proportional to $|A_1|^2$, $\tau\to\nu_\tau K^- K^{*0}$ receives contributions only from the region of $M_{KK^*}<m_\tau$. Our mock data implies $\sim 60\,\%$ of the $\bar{B}^0\to D^+ K^- K^{*0}$ rate comes from $M_{KK^*}<m_\tau$. The dominance of near threshold contributions suggested by $\bar{B}^0\to D^+ K^- K^{*0}$ data translates to a large $\tau\to\nu_\tau K^- K^{*0}$. Thus, to reduce $\mathcal{B}(\tau\to\nu_\tau K^- K^{*0})$ from $\sim 0.5\,\%$ down to $\sim 0.2\,\%$, one needs to reduce the relative contribution coming from near threshold. We illustrate this by the dot-dash line in Fig. 4, where only $\sim 32\,\%$ of the rate comes from $M_{KK^*}\leqslant m_\tau$ and the peak is shifted toward higher t. This would have given the correct rates $\mathcal{B}(\tau\to\nu_\tau K^- K^{*0})\sim 2.1\times 10^{-3}$ and $\mathcal{B}(\bar{B}^0\to D^+ K^- K^{*0})\sim 8.8\times 10^{-4}$, but seems to disagree with the mock $\bar{B}^0\to D^+ K^- K^{*0}$ spectrum.

Recall, however, the comparison between the predicted spectrum of $D^+ K^- K^0$ with that of $D^0 K^- K^0$ in Ref. [3]. Due to the additional $B\to KK$ transition mechanism that is asymptotically $1/t^2$, the $D^0 K^- K^0$ spectrum has a peak closer to the threshold (~ 250 MeV above threshold) than that of $D^+ K^- K^0$ (~ 600 MeV above threshold). Since the mock data used in the present work is generated from published data that *combines* those of $D^+ K^- K^{*0}$, $D^{*+} K^- K^{*0}$, $D^0 K^- K^{*0}$, and $D^{*0} K^- K^{*0}$, it is conceivable that the real data for $\bar{B}^0\to D^+ K^- K^{*0}$ could be somewhat closer to the dot-dash line in Fig. 4, which peaks at ~ 400 MeV above threshold. In other words, the peak near the threshold of Fig. 3 (or Fig. 4) could be due to the $D^{(*)0} K^- K^{*0}$ modes, whereas the apparent peak at ~ 2 GeV in Fig. 3 (which we removed in Fig. 4) might be some hint of the behavior of the $D^{(*)+} K^- K^{*0}$ modes. The situation can be clarified by separating $D^+ K^- K^{*0}$ and $D^0 K^- K^{*0}$ with more data. We note further from Fig. 5 that $|A_1^{KK^*}(q^2=(1.5\ \mathrm{GeV})^2)|\simeq 1.3$ is larger than $|F_1^{KK}(q^2=(1.5\ \mathrm{GeV})^2)|\simeq 0.7$ as fitted from kaon EM data Ref. [3]. This gives further support of our conjecture that contamination of $B^-\to D^{(*)0} K^- K^{*0}$ in the mock data could be responsible for the enhancement of our $\tau\to\nu_\tau K^- K^{*0}$ rate.

From the point of view of extracting the timelike $K^- K^{*0}$ axial A_1 form factor, $\tau\to\nu_\tau K^- K^{*0}$ is better because the production of KK^* is purely proportional to A_1. However, it has limited range in momentum transfer. In contrast, the $\bar{B}^0\to D^+ K^- K^{*0}$ mode allows us to probe higher t, but one has the associated factor $a_1 F_1^{BD}$ [see Eq. (12)], which means one is further subject to possible corrections to factorization. We have assumed certain values for $a_1 F_1^{BD}$ to extract A_1. A more appropriate way to proceed would be to treat A_1 and $a_1 F_1^{BD}(q^2)$ on equal footing, both as suitably parametrized functions to be determined from data. To be able to do so, one needs further independent data, such as an analysis of $\bar{B}\to D\rho\pi$ decay aimed at extracting $\bar{B}\to D a_1(1260)$, which should be performed in a similar way to our $\bar{B}^0\to D^+ K^- K^{*0}$ study, including angular analysis and proper parametrization of π-ρ axial form factor that respects PQCD for large $M_{\rho\pi}$. There is, of course, the need for concurrent check on validity of factorization. This may then involve extraction of $F_1^{BD}(q^2)$ from $\bar{B}^0\to D^+\ell^-\nu$.

Our result reveals that the contribution from the $a_1(1260)$ resonance ($\sim 9\,\%$) is much smaller than that from the nonresonant part ($\sim 54\,\%$). While this underlines the importance of nonresonant part, the smallness of the $a_1(1260)$ resonance contribution is curious. Recall that in the $\bar{B}^0\to D^+ K^- K^0$ decay we have ρ-resonance contribution up to $40\,\%$ [3]. It should be pointed out that, through $SU(3)$ relations, the ρ resonance contribution in F_1^{KK} is highly constrained by the well-measured ϕ resonance contribution in kaon EM data [3]. It is not clear if the smallness of the a_1 resonance contribution is an artifact of having only one resonant term. On the other hand, the smallness of $R\sim R_{\mathrm{CLEO}}<10\,\%$ seems to support a suppressed $a_1(1260)$-resonance contribution. It is interesting to see that, if we follow Ref. [1] to take the ratio between the rate contributed from $a_1(1260)$ alone (9 % of the total) and the rate of $\bar{B}^0\to D^+ a_1^-(1260)$ from Ref. [11], we obtain $R\sim 1.3\,\%$, which is about 9 % of the Belle result $R_{\mathrm{Belle}}\sim 15\,\%$. The discrepancy could be due to the breakdown of the narrow width limit and the physical fact of $m_{KK^*}<m_{a_1}$, which are essential for R_{Belle} to be identical with R defined in Eq. (21).

The case of $\bar{B}^0\to D^+\rho^0\pi^-$ is somewhat better in the sense that $\rho\pi$ is dominated by the a_1 resonance. However, there are many resonances that decay to the $\rho\pi$ final state. One can extract $\bar{B}\to D a_1(1260)$ rate by suitably considering these resonant and nonresonant contributions. The branching fractions of $\mathcal{B}[\bar{B}^0\to D^+ a_1^-(1260)]=(0.60\pm 0.22\pm 0.24)\,\%$ and $\mathcal{B}[B^-\to D^0 a_1^-(1260)]=(0.45\pm 0.19\pm 0.31)\,\%$ were obtained by an analysis of $\bar{B}\to D\pi\pi\pi$ decays based on $\sim 200\ \mathrm{pb}^{-1}$ of data [12]. The large systematic error is dominated by uncertainties in fitting and are estimated by considering alternate backgrounds. The mass and the width of $a_1(1260)$ were taken as *a priori* in the extraction, which may no longer be appropriate when the data has improved by more than three orders of magnitude by the B factories. To reduce the effect caused by uncertain properties such as the width and subdecay modes of $a_1(1260)$, an amplitude that takes into account as complete substructures of $a_1(1260)$ as possible is needed. Furthermore, as we have seen from the fit to the $\bar{B}^0\to D^+ K^- K^{*0}$ data, a nonresonant part that respects PQCD at higher t may contribute significantly to the results, which must also be taken into account to complete the construction of the amplitude. Of course, the cost would be to boost the number of fit parameters, but fortunately one now has enormous amount of data.

As noted in the end of the previous section, the $a_1(1260)$ contribution depends on g_s and Γ_{a_1} roughly through the ratio g_s/Γ_{a_1}. Thus, $\bar{B}^0\to D^+ K^- K^{*0}$ mode is not so powerful for determining the resonance parameters. One needs independent determination of these parameters, especially Γ_{a_1} from other sources. Therefore, it appears that, to extract the axial

K-K^* form factor A_1 and understand properly the $a_1(1260)$ component, one needs to perform a combined analysis of $\bar{B}^0 \to D^+ K^- K^{*0}$, $D^+ \rho^0 \pi^-$, $D^+ \ell^- \nu$, and $\tau \to \nu_\tau K^- K^{*0}$.

In conclusion, based on what is revealed by 29.4 fb^{-1} data from Belle, we have illustrated how to extract the time-like K^--K^{*0} axial form factor $A_1(M^2_{KK^*})$ from $\bar{B}^0 \to D^+ K^- K^{*0}$ data. The method can be easily generalized to other form factors by angular analysis when more data becomes available. With >300 fb^{-1} data already accumulated by KEKB and PEP-II, if the case for factorization in such three-body B decays is further strengthened, the B Factories may be promising for the study of hadronic form factors that may be otherwise inaccessible. Hadronic form factors have played an instrumental role in the formulation of nuclear and particle physics, and further insight may perhaps be gained from quantities such as the K-K^* axial form factor. Our study already indicates that the nonresonant contribution, needed to account for large t behavior, is rather significant. The current discussion also illustrates how nucleon axial form factors can be extracted from $B^0 \to D^{(*)-} p\bar{n}$ decay once the spectrum becomes available.

ACKNOWLEDGMENTS

We thank A. Drutskoy, H.-C. Huang, and H.-n. Li for discussions. This work is supported in part by the National Science Council of R.O.C. under Grants No. NSC-92-2112-M-002-024 and No. NSC-92-2811-M-001-054, the MOE CosPA Project, and the BCP Topical Program of NCTS.

[1] Belle Collaboration, A. Drutskoy *et al.*, Phys. Lett. B **542**, 171 (2002).
[2] CLEO Collaboration, D.M. Asner *et al.*, Phys. Rev. D **61**, 012002 (2000).
[3] C.-K. Chua, W.-S. Hou, S.-Y. Shiau, and S.-Y. Tsai, Phys. Rev. D **67**, 034012 (2003).
[4] If $J>1$ components for $K^- K^0$ is extracted in the future, one would have to go beyond factorization to account for it.
[5] CLEO Collaboration, S. Anderson *et al.*, Phys. Rev. Lett. **86**, 2732 (2001).
[6] C.-K. Chua, W.-S. Hou, and S.-Y. Tsai, Phys. Rev. D **65**, 034003 (2002).
[7] Belle Collaboration, K. Abe *et al.*, Phys. Rev. Lett. **89**, 151802 (2002).
[8] H.-Y. Cheng and K.-C. Yang, Phys. Rev. D **66**, 094009 (2002).
[9] D. Melikhov and B. Stech, Phys. Rev. D **62**, 014006 (2000).
[10] S.J. Brodsky and G.R. Farrar, Phys. Rev. D **11**, 1309 (1975).
[11] Particle Data Group Collaboration, K. Hagiwara *et al.*, Phys. Rev. D **66**, 010001 (2002).
[12] CLEO Collaboration, D. Bortoletto *et al.*, Phys. Rev. D **45**, 21 (1992).